

Inhibitory Effect of Tricalcium Phosphate Sintered at Different Temperatures on Human Breast Cancer Cell Line MCF-7

Mehdi Rahmanian¹, Seyed Morteza Naghib^{1,2,*}, Amir Seyfoori^{1,3}, Ali Akbar Zare⁴, Hasan Sanati¹, Keivan Majidzadeh-A⁴

¹ Breast Cancer Research Center, ACECR, Tehran, Iran

² Nanotechnology Department, School of New Technologies, Iran University of Science and Technology (IUST), Tehran, Iran

³ School of Metallurgy and Materials engineering, College of Engineering, University of Tehran, Tehran, Iran

⁴ Breast Cancer Genetics Department, Breast Cancer Research Center, ACECR, Tehran, Iran

* Corresponding author: Seyed Morteza Naghib, Nanotechnology Department, School of New Technologies, Iran University of Science and Technology (IUST), P.O. Box 16846-13114, Tehran, Iran. E-mail: naghib@iust.ac.ir

DOI: 10.21859/mci-01012

Submitted: 7 March 2016

Revised: 22 July 2016

Accepted: 1 August 2016

ePublished: 08 September 2016

Keywords:

Tricalcium Phosphate

Nanoparticles

Therapeutics

Abstract

Introduction: Achievement of new drugs with minimal side effects is an important goal in the cancer treatment due to irreversible side effects of conventional drugs. Tricalcium phosphates as natural bone components have unique characteristics including excellent biocompatibility, high biosorption and superior bioactivity. This research aimed at investigating the inhibitory effect of tricalcium phosphate (TCP) sintered at different temperatures.

Methods: TCP nanoparticles (nTCP) were sintered at three temperatures of 700°C, 900°C and 1000°C, and their structural characterization was examined. Heat treatment of TCP at 900°C was found optimal due to its morphological properties, such as particle size and its crystallinity. The inhibitory effect of optimized nTCP sintered at 900°C was surveyed through *in vitro* tests.

Results: Cell culture assay studies exhibited that such effect depended on the concentration of nTCP. Moreover, the results depicted that the effect was 80%, which could be attributed to the 50 mg.L⁻¹ dose of nTCP.

Conclusions: In lower concentrations, higher inhibitory effect of nTCP was observed. In comparison with hydroxyapatite, at low concentrations, anti-cancer properties of TCP were far greater than other calcium phosphates.

© 2016. Multidisciplinary Cancer Investigation

INTRODUCTION

Materials based on calcium phosphates (CP) are the main mineral constituents of human hard tissues, such as bones and teeth [1-5]. Calcium phosphate bio-ceramics, including hydroxyapatite (HA) and tricalcium phosphates (TCP) as the most common types, are increasingly investigated as bone repair materials due to their similarity to the mineral component of the bone tissue [6-8]. Recently, synthetic CP nanostructures have attracted many researchers, owing to their good biocompatibility, excellent bioactivity, adequate biodegradability, and high affinity to polymers and biomacromolecules, as well as large osteogenic potential [9-13]. So far, it has been well expressed that CP nanostructures can increase the growth of bones through

osteoconduction mechanism, without causing any local or systemic toxicity, inflammation, or foreign body response [14]. In comparison with CP microstructures, CP nanostructures have unique characteristics such as improved hardness and fracture resistance, amended bone binding properties, promoted drug loading capacity and enhanced solubility [15].

Conventional medications for cancer treatment entail irreversible side effects in numerous cases, so achieving new drugs with minimal side effects is an important goal in the cancer treatment arena [16]. Recently, the inhibitory effect of hydroxyapatite nanoparticles, an important component of calcium phosphate in natural bones, on the proliferation of cancer cells has been investigated [17-20]. The results of *in vitro* and *in vivo* studies have shown that hydroxyapatite nanoparticles have been able to prevent growth in some

cancer cells, including some breast cancer cell lines [19, 20]. Furthermore, recent observations have depicted that nano-hydroxyapatite has had very little inhibitory effect on the proliferation of healthy cells [18].

Previous studies demonstrated that applying heat treatments on ceramics can generate the energy needed to form crystalline CPs [21]. These crystalline structures caused a significant reduction in dissolution rate as compared with the amorphous structures [22]. This research claims to be the first study on the MCF-7 inhibitory effect of sintered crystalline CPs.

Here, TCP was sintered at three temperatures including 700°C, 900°C and 1000°C, and the structural characterization of the heat-treated samples was investigated. Morphology and physicochemical properties of the samples were studied via scanning electron microscopy (SEM), Fourier transform infrared spectroscopy (FTIR), and X-ray powder diffraction (XRD). Next, the inhibitory effects of TCP nanoparticles (nTCP) on the growth and proliferation of MCF-7 breast cancer cell lines were studied, and the inhibitory effect of optimized nTCP sintered at 900°C was surveyed through *in vitro* tests.

METHODS

Materials

TCP ($\text{Ca}_3(\text{PO}_4)_2$) was purchased from Merck Co. (Germany). MCF-7 cell line was also presented by the Pasture Institute of Iran.

Heat Treatment

Five grams of TCP nano-powder was sintered at 700°C, 900°C and 1000°C for one hour, and cooled to room temperature. The largest amount of TCP was obtained after heat treatment at 900°C (4.8 g). Then, the nTCP was prepared for being used as an inhibitory drug.

Cell Culture

The MCF-7 cells were cultured in a 25 cm² flask in a medium containing Dulbecco's Modified Eagle's Medium (DMEM/Gibco), 10% FBS, 100 U/mL penicil-

lin, and 100 µg/mL streptomycin at 37°C with 5% CO₂, 95% air and complete humidity. Once they reached ~90% confluency, they were detached using 0.05% trypsin/EDTA, and counted by means of trypan blue and hemocytometer. These cells were then resuspended at a concentration of 1×10^5 cells and added into a 96-well plate. After 24 hours, when the cells deposited at the plate bottom, the culture media were replaced with the treatment media. All the treatment media contained 90% culture medium, 10% fetal bovine serum (FBS), and different amounts of TCP at final concentrations of 50 mg.L⁻¹, 100 mg.L⁻¹, 150 mg.L⁻¹ and 200 mg.L⁻¹.

MTT Assay for Evaluating Cell Viability

After 48 hours, the MTT solution was prepared at 1 mg/mL in phosphate buffered saline (PBS), and filtered through a 0.2 µm filter. Then, 22 µL of MTT plus 200 µL of DMEM were added into each well, except for the cell-free blank wells. The cells were incubated for four hours at 37°C with 5% CO₂, 95% air and complete humidity. After four hours, the MTT solution was removed and replaced with 100 µL of DMSO. The plate was further incubated for 15 minutes at room temperature, and the optical density (OD) of the wells was determined using a plate reader (Biotek) at a test wavelength of 570 nm and a reference wavelength of 630 nm.

RESULTS

Morphology evaluation of materials and biospecies is of key significance in characterization of biomaterials. The morphology of the TCP nano-powder sintered at different temperatures is shown in Figure 1. Figure 2 shows the XRD patterns of the sample, illustrating the pattern of TCP nanostructures sintered at 700°C, 900°C and 1000°C. Moreover, the corresponding FTIR absorption spectra of the nanoceramic powders sintered at 900°C are depicted in Figure 3. The inhibitory effects of nTCP on the MCF-7 cancer cell proliferation were compared at the concentrations of 50 mg.L⁻¹, 100 mg.L⁻¹, 150 mg.L⁻¹ and 200 mg.L⁻¹. Results displayed in Figure 4 affirm that nTCP can inhibit the proliferation of human cancer cells.

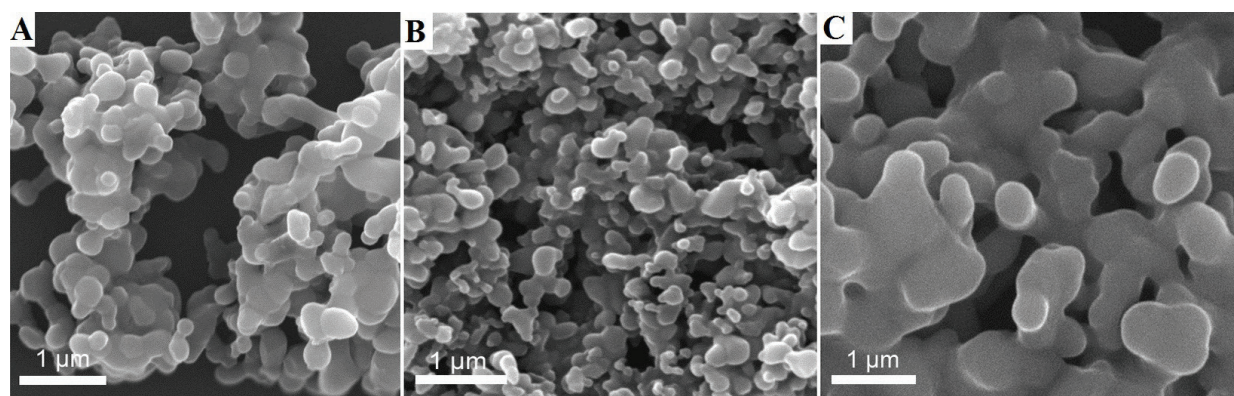


Figure 1: SEM Micrograph of TCP Powders Sintered at A) 1000°C, B) 900°C, and C) 700°C (pH = 7.4)

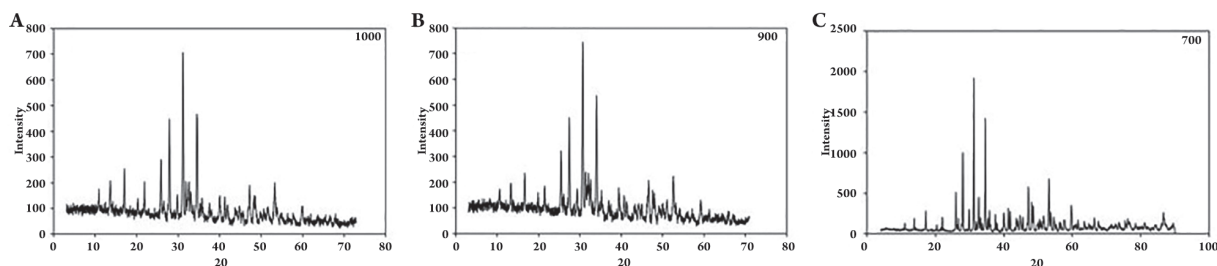


Figure 2: XRD Pattern of the TCP Nano-Powder at A) 1000°C, B) 900°C, and C) 700°C (pH = 7.4)

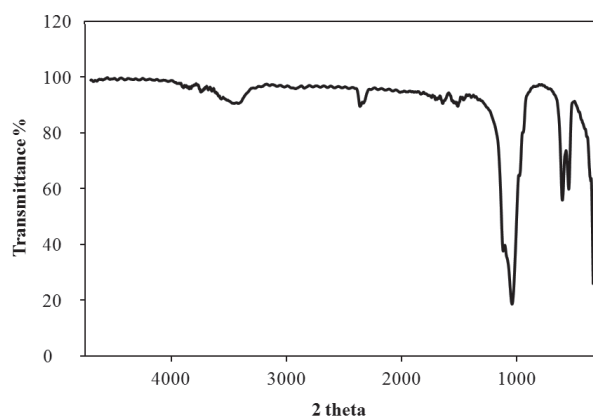


Figure 3: FTIR Absorption Spectra of the TCP Nano-Powder Sintered at 900°C

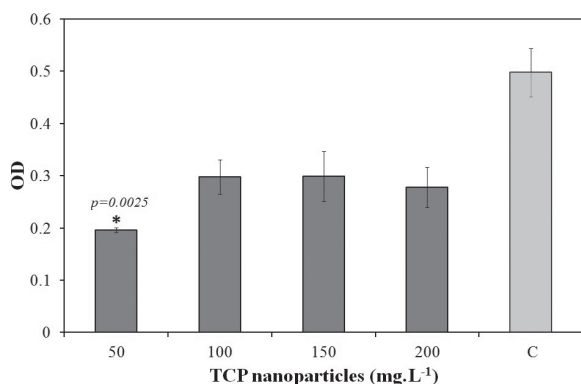


Figure 4: Concentration Effects of TCP Nanoparticles on MCF-7 Breast Cancer Cell Proliferation. All the nanoparticles were used at the concentrations of 50 mg.L⁻¹, 100 mg.L⁻¹, 150 mg.L⁻¹ and 200 mg.L⁻¹ respectively in phosphate buffer solution (P = 0.0025, P < 0.05).

DISCUSSION

As can be seen in the Figure 1, the nano-powder sintered at 700°C and 1000°C is highly agglomerated, which may be due to grains growth and creation of new grain boundaries. The TCP nanostructures heat-treated at 900°C were almost spherical, and the observed particle size was approximately 70 nm. It seems that sintering TCP at 900°C was optimal due to its morphological properties such as particle size.

The characteristic PO₄³⁻ and OH absorption bands of HA were observed in the sintered sample, along with the additional broad bands at 1640 cm⁻¹ and 3430 cm⁻¹ from the adsorbed H₂O (Figure 3). The weak absorption peak at 880 cm⁻¹ was assigned to the P–O–H vibration in the HPO₄²⁻ group existing in TCP. The C–O vibration in the CO₃²⁻ group can also corroborate to this absorption band. In the sample calcined at 900°C, the OH absorption band disappeared and the spectrum obtained was characteristic of TCP (Figure 3). When increasing the sintering temperature, the PO₄³⁻ vibration peaked at 603 and 568 cm⁻¹ gradually merged. The FTIR spectrum of the powders calcined at 700°C and 1000°C resembled that of TCP, which conformed to the previous XRD results.

As can be seen in Figure 4, the inhibitory effects of nTCP on breast cancer cell proliferation were far more extensive than controls. The inhibitory effects of different concentrations of TCP on breast cancer cell proliferation ranged from 25% to 79% depending on the applied dosage. The cytotoxic effects of hydroxyapatite concentration as a calcium phosphates derivative on the proliferation of cancer cells has been investigated previously [19, 20]. Moreover, previous studies demonstrated serious disagreements over inhibition degree among different cancer cell lines as well as among normal cell lines. The cell-toxic and inhibitory effects of nTCP on cancer cell growth also depend on the related treatment time [18].

The particle size and the dosage-dependent inhibitory effects of nHAP on cancer cells have been established [18]. Moreover, with smaller nHAP levels, higher degrees of inhibition were observed [18, 20]. At the concentration of 50 mg.L⁻¹, the inhibitory effect of TCP particles on MCF-7 cells significantly increased to about 80%. The effect diminished from about 79% to about 25% with dosage increase (50 mg.L⁻¹, 100 mg.L⁻¹, 150 mg.L⁻¹ and 200 mg.L⁻¹). As a whole, nanomaterials such as nanoparticles and nanotubes could enter cancer cells and reach cytoplasm and different organelles that depended on different characteristics of the nanomaterials. As it has been verified, nTCP possesses two different binding sites on the crystal surface, namely C (Ca²⁺) site, arranged on ac or bc crystal faces for binding the acidic groups of the biomolecules, and P PO₄³⁻ site, arranged hexagonally on the ab crystal face for attachment

to the basic groups of the biomolecules. Numerous negatively-charged groups and ions on the cancer cell surface generate higher negative charge of cancer cells than other cells. This phenomenon mainly depends on the sialic acid residues and other materials secreted from the apical surface of the plasma membrane [18].

To summarize, the present study investigated the structural characterization of sintered samples, and their morphology and physicochemical properties were studied via SEM, FTIR, and XRD. The inhibitory effects of nTCP on the growth and proliferation of MCF-7 breast cancer cell lines were also studied. Moreover, the same effect was evaluated for nTCP sintered at 900°C through *in vitro* tests. The results obtained indicate that a higher dose of nTCP induced oxidative stress on the breast cancer cell, MCF-7, which in turn led to apoptotic-like conditions.

ACKNOWLEDGMENTS

This research was financially supported by Breast Cancer Research Center (BCRC) of Iran. The authors would like to acknowledge the products and services provided by BCRC that facilitated this research, including experimental setups.

CONFLICT OF INTEREST

The authors declare that there are no competing financial interest.

REFERENCES

1. Batchelar DL, Davidson MT, Dabrowski W, Cunningham IA. Bone-composition imaging using coherent-scatter computed tomography: assessing bone health beyond bone mineral density. *Med Phys*. 2006;33(4):904-15. DOI: [10.1118/1.2179151](https://doi.org/10.1118/1.2179151) PMID: [16696465](https://pubmed.ncbi.nlm.nih.gov/16696465/)
2. Malmberg P, Nygren H. Methods for the analysis of the composition of bone tissue, with a focus on imaging mass spectrometry (TOF-SIMS). *Proteomics*. 2008;8(18):3755-62. DOI: [10.1002/pmic.200800198](https://doi.org/10.1002/pmic.200800198) PMID: [18780399](https://pubmed.ncbi.nlm.nih.gov/18780399/)
3. Marten A, Fratzl P, Paris O, Zaslansky P. On the mineral in collagen of human crown dentine. *Biomaterials*. 2010;31(20):5479-90. DOI: [10.1016/j.biomaterials.2010.03.030](https://doi.org/10.1016/j.biomaterials.2010.03.030) PMID: [20399496](https://pubmed.ncbi.nlm.nih.gov/20399496/)
4. Sadat-Shojai M, Khorasani MT, Dinpanah-Khoshdargi E, Jamshidi A. Synthesis methods for nanosized hydroxyapatite with diverse structures. *Acta Biomater*. 2013;9(8):7591-621. DOI: [10.1016/j.actbio.2013.04.012](https://doi.org/10.1016/j.actbio.2013.04.012) PMID: [23583646](https://pubmed.ncbi.nlm.nih.gov/23583646/)
5. Ansari M, Naghib SM, Moztafzadeh F, Salati A. Synthesis and Characterization of Hydroxyapatite Calcium Hydroxide for Dental Composites. *Ceram-Silikaty*. 2011;55(2):123-126.
6. Enderle R, Gotz-Neunhoeffer F, Gobbels M, Muller FA, Greil P. Influence of magnesium doping on the phase transformation temperature of beta-TCP ceramics examined by Rietveld refinement. *Biomaterials*. 2005;26(17):3379-84. DOI: [10.1016/j.biomaterials.2004.09.017](https://doi.org/10.1016/j.biomaterials.2004.09.017) PMID: [15621226](https://pubmed.ncbi.nlm.nih.gov/15621226/)
7. Hench LL. Bioceramics. *J America Ceramic Society*. 2005;81(7):1705-28. DOI: [10.1111/j.1151-2916.1998.tb02540.x](https://doi.org/10.1111/j.1151-2916.1998.tb02540.x)

8. Kamitakahara M, Ohtsuki C, Miyazaki T. Review paper: behavior of ceramic biomaterials derived from tricalcium phosphate in physiological condition. *J Biomater Appl*. 2008;23(3):197-212. DOI: [10.1177/0885328208096798](https://doi.org/10.1177/0885328208096798) PMID: [18996965](https://pubmed.ncbi.nlm.nih.gov/18996965/)
9. Frede A, Neuhaus B, Klopffleisch R, Walker C, Buer J, Muller W, et al. Colonic gene silencing using siRNA-loaded calcium phosphate/PLGA nanoparticles ameliorates intestinal inflammation *in vivo*. *J Control Release*. 2016;222:86-96. DOI: [10.1016/j.jconrel.2015.12.021](https://doi.org/10.1016/j.jconrel.2015.12.021) PMID: [26699423](https://pubmed.ncbi.nlm.nih.gov/26699423/)
10. Gao X, Lan J, Jia X, Cai Q, Yang X. Improving interfacial adhesion with epoxy matrix using hybridized carbon nanofibers containing calcium phosphate nanoparticles for bone repairing. *Mater Sci Eng C Mater Biol Appl*. 2016;61:174-9. DOI: [10.1016/j.msec.2015.12.033](https://doi.org/10.1016/j.msec.2015.12.033) PMID: [26838838](https://pubmed.ncbi.nlm.nih.gov/26838838/)
11. Karimi M, Hesarakhi S, Alizadeh M, Kazemzadeh A. Synthesis of calcium phosphate nanoparticles in deep-eutectic choline chloride-urea medium: Investigating the role of synthesis temperature on phase characteristics and physical properties. *Ceramics Int*. 2016;42(2):2780-88. DOI: [10.1016/j.ceramint.2015.11.010](https://doi.org/10.1016/j.ceramint.2015.11.010)
12. Qian J, Ma J, Su J, Yan Y, Li H, Shin JW, et al. PHBV-based ternary composite by intermixing of magnesium calcium phosphate nanoparticles and zein: In vitro bioactivity, degradability and cytocompatibility. *Europ Polym J*. 2016;75(3):291-302. DOI: [10.1016/j.eurpolymj.2015.12.026](https://doi.org/10.1016/j.eurpolymj.2015.12.026)
13. Zhang J, Sun X, Shao R, Liang W, Gao J, Chen J. Corrigendum to "Polycation liposomes combined with calcium phosphate nanoparticles as a non-viral carrier for siRNA delivery" [*J Drug Deliv Sci Technol*. 30PA (2015) 575-588]. *J Drug Deliv Sci Technol*. 2016;31:187. DOI: [10.1016/j.jddst.2016.01.006](https://doi.org/10.1016/j.jddst.2016.01.006)
14. Mi P, Kokuryo D, Cabral H, Kumagai M, Nomoto T, Aoki I, et al. Hydrothermally synthesized PEGylated calcium phosphate nanoparticles incorporating Gd-DTPA for contrast enhanced MRI diagnosis of solid tumors. *J Control Release*. 2014;174:63-71. DOI: [10.1016/j.jconrel.2013.10.038](https://doi.org/10.1016/j.jconrel.2013.10.038) PMID: [24211705](https://pubmed.ncbi.nlm.nih.gov/24211705/)
15. Koshkaki MR, Ghassai H, Khavandi A, Seyfoori A, Molazemhosseini A. Effects of formaldehyde solution and nanoparticles on mechanical properties and biodegradation of gelatin/nano β -TCP scaffolds. *Iran Polymer J*. 2013;22(9):653-64. DOI: [10.1007/s13726-013-0164-0](https://doi.org/10.1007/s13726-013-0164-0)
16. Overall CM, Kleinfeld O. Validating matrix metalloproteinases as drug targets and anti-targets for cancer therapy. *Nat Rev Cancer*. 2006;6(3):227-39.
17. Choi S, Coonrod S, Estroff L, Fischbach C. Chemical and physical properties of carbonated hydroxyapatite affect breast cancer cell behavior. *Acta Biomater*. 2015;24:333-42. DOI: [10.1016/j.actbio.2015.06.001](https://doi.org/10.1016/j.actbio.2015.06.001) PMID: [26072364](https://pubmed.ncbi.nlm.nih.gov/26072364/)
18. Han Y, Li S, Cao X, Yuan L, Wang Y, Yin Y, et al. Different inhibitory effect and mechanism of hydroxyapatite nanoparticles on normal cells and cancer cells *in vitro* and *in vivo*. *Sci Rep*. 2014;4:7134. DOI: [10.1038/srep07134](https://doi.org/10.1038/srep07134) PMID: [25409543](https://pubmed.ncbi.nlm.nih.gov/25409543/)
19. Meena R, Kesari KK, Rani M, Paulraj R. Effects of hydroxyapatite nanoparticles on proliferation and apoptosis of human breast cancer cells (MCF-7). *J Nanoparticle Res*. 2012;14(2):1-11. DOI: [10.1007/s11051-011-0712-5](https://doi.org/10.1007/s11051-011-0712-5)
20. Morgan MP, Cooke MM, Christopherson PA, Westfall PR, McCarthy GM. Calcium hydroxyapatite promotes mitogenesis and matrix metalloproteinase expression in human breast cancer cell lines. *Mol Carcinog*. 2001;32(3):111-7. DOI: [10.1002/mc.1070](https://doi.org/10.1002/mc.1070) PMID: [11746823](https://pubmed.ncbi.nlm.nih.gov/11746823/)
21. Ong JL, Lucas LC. Post-deposition heat treatments for ion beam sputter deposited calcium phosphate coatings. *Biomaterials*. 1994;15(5):337-41. DOI: [10.1016/0142-9612\(94\)90245-3](https://doi.org/10.1016/0142-9612(94)90245-3) PMID: [8061124](https://pubmed.ncbi.nlm.nih.gov/8061124/)
22. Yang Y, Kim KH, Ong JL. A review on calcium phosphate coatings produced using a sputtering process--an alternative to plasma spraying. *Biomaterials*. 2005;26(3):327-37. DOI: [10.1016/j.biomaterials.2004.02.029](https://doi.org/10.1016/j.biomaterials.2004.02.029) PMID: [15262475](https://pubmed.ncbi.nlm.nih.gov/15262475/)